

Uncertainty in Impact Identification Applied to a Commercial Wind Turbine Blade

Raymond M Bond¹, Douglas E Adams²

^{1,2} *Purdue University, West Lafayette, IN, 47906, USA*

rmbond@purdue.edu

deadams@purdue.edu

Abstract

This work evaluates the uncertainty of impact force and location estimates using an entropy-based impact identification algorithm applied to a commercial wind turbine blade. The effects of sensor placement, measurement directions and distance between impacts and sensor locations are studied. Results show that impacts to a 35m long wind turbine blade can be accurately located using a single tri-axial accelerometer regardless of sensor location. Uncertainties in impact force estimates are consistent across sensor locations. When omitting acceleration information in the spanwise direction, the bias and variance of force estimates is consistent, but when a single channel of acceleration data is used, both increase somewhat. Impact force identification error was found to be uncorrelated with the distance between the impact and sensor location. The entropy of the estimated force time history, an indicator of the impulsivity of the estimate, was found to be a good indicator of the quality of force estimate. The bias and variance of impact force estimation error was found to be directly correlated with the entropy of the impact force estimate. When considering validation test data from all possible sensor configurations, the entropy of the recreated force estimates was a better indicator of the force magnitude prediction interval than was the specific sensor configuration. By classifying impact force estimates based upon entropy values, impact force prediction intervals were more precisely determined than when all validation impact data were considered at once.

1. Introduction

Impact damage is a significant concern for most large composite structures because this type of damage is often

below the surface and not evident from visual inspection. Composite damage mechanisms such as delaminations, substructure disbonds and core crushing can substantially reduce the strength of the structure without providing a clear visual indication. Inspection for this type of damage is often very time consuming and requires multiple inspection techniques to accurately identify the location and extent of these numerous damage mechanisms (Hayman, Wedel-Heinen, & Brondsted, 2008). Inspection of large rotor blades is particularly expensive and challenging, due to the size and inaccessibility of these blades. The inspection burden could be significantly alleviated by identifying the location and magnitude of applied impact loads. However, in order to make an informed maintenance decision based on these types of impact estimates, the associated uncertainty must be well understood. To this end, this work applies an entropy-based impact identification technique to a commercial wind turbine blade, and then evaluates the performance and uncertainty of impact location and force estimates.

Damaging impact loads are a concern for wind turbine blades both while in operation and during transport (Cripps, 2011; Veritas, 2006). Some examples of impact loads in operation are hail, bird strikes, or ice shedding from other blades. One study found that 7% of unforeseen malfunctions in 1.5MW wind turbines operating in Germany have been attributed to rotor blade problems, with an average down time of four days per failure (Hahn, Durstewitz, & Rohrig, 2007). Unforeseen repairs on wind turbines are especially costly, as these repairs are around 500% more expensive than regularly scheduled maintenance (Adams, White, Rumsey, & Farrar, 2011). An impact load estimation technique such as the one presented here has the potential to provide maintainers the information they need to limit the progression of damage by way of prompt repairs, schedule maintenance in advance, and track the loading history of blades to identify problematic trends.

Raymond Bond et al. This is an open-access article distributed under the terms of the Creative Commons Attribution 3.0 United States License, which permits unrestricted use, distribution, and reproduction in any medium, provided the original author and source are credited.

Impact identification methods have been widely studied (see, for example, (H. Inoue & Reid, 2001; Inoue, Kishimoto, Shibuya, & Koizumi, 1992; Hu, Matsumoto, Nishi, & Fukunaga, 2007; Stites, 2007; Yoder & Adams, 2008; Wang & Chiù, 2003)). These techniques are generally categorized as model-based techniques, based on an underlying model of the system, and artificial neural network based techniques, which are based on representative response training data and computational algorithms. Although neural network based techniques can be effective at locating impacts using a large array of sensors, model-based techniques are better suited to load estimation, even in sparse sensing configurations. For instance, other work from our research group (Budde, Yoder, Adams, Meckl, & Koester, 2009; Budde, 2010; Stites, Escobar, White, Adams, & Triplett, 2007; Stites, 2007; Yoder & Adams, 2008) has shown the ability to estimate impact load and position using a single sensor on filament-wound rocket motor casings and helicopter blades. This work builds on these previous efforts by developing an impact identification algorithm capable of monitoring very large and/or non-uniform structures with a single sensor.

2. Theory

This impact identification algorithm consists of two major steps: (1) estimating a set of potential impact forces assuming each of the possible input degrees of freedom, and (2) determining which of these force estimates most likely corresponds to the actual forcing location. The first step of this process is the same as that presented in (Yoder & Adams, 2008; Stites, 2007; Stites et al., 2007; Budde et al., 2009); the distinction between this algorithm and these other works is the method used to determine the likely impact location.

Estimated impact loads at each potential input degree of freedom are found by formulating and solving an overdetermined inverse problem based on experimentally estimated frequency response functions and measured responses. Given N_i input degrees of freedom and N_o output degrees of freedom, the response, $\{X(j\omega)\}$, can be expressed in terms of the frequency response function matrix, $[H(j\omega)]$, and forcing function, $\{F(j\omega)\}$, as follows:

$$\{X(j\omega)\}_{(N_o \times 1)} = [H(j\omega)]_{(N_o \times N_i)} \{F(j\omega)\}_{(N_i \times 1)} \quad (1)$$

For practical implementations, the number of response channels would be significantly fewer than the number of input degrees of freedom, that is, $N_o \ll N_i$. With this constraint on the system configuration, the inverse problem of solving for $F(j\omega)$ based on $H(j\omega)$, $X(j\omega)$ and the relationship given in (1) is underdetermined with an infinite number of solutions. To reliably estimate the

impact forces based on measured data, an overdetermined inverse problem is ideal in order to minimize the effects of measurement noise and error in the estimated frequency response functions. By assuming that the forcing function acts at a single degree of freedom, k , (1) can be re-written as follows:

$$\{X(j\omega)\}_{(N_o \times 1)} = \{H_k(j\omega)\}_{(N_o \times 1)} F_k(j\omega) \quad (2)$$

With the force-response relationship in this form, the force can be determined given the frequency response function and any (non-zero) number of response channels. This inverse problem is overdetermined when more than one response channel is available. The linear least squares estimate of the forcing function at a particular frequency, $F_k(j\omega)$, is found by pre-multiplying 2 by the pseudoinverse of the frequency response function matrix at that frequency, $\{H_k(j\omega)\}^+$. Other numerical methods could also be used to solve for the least squares solution, but the pseudoinverse approach is advantageous for real-time impact monitoring because the computationally intensive portion of the solution procedure, calculating the pseudoinverse, is done prior to monitoring the structure for impacts, leaving only matrix multiplication to be done in real time.

Because the actual location of impact is unknown, the impact force must be estimated at each of the possible input degrees of freedom, and then the force estimates are analyzed to determine which of these force estimates most likely corresponds to the actual impact location. To determine which force estimate corresponds to the true location, the estimated force time histories for each location are analyzed to find which best matches the assumption of an impulsive impact force. The impulsivity of the recreated force time histories is quantified by evaluating the entropy of the impact force time histories.

Entropy in the context of information theory, is a measure of the average quantity of information contained in each event, in this case, in each sample of signal. The total information of a signal is defined as the minimum number of bits required to completely describe the signal. A purely random signal has the highest possible entropy, and a completely uniform signal has zero entropy. For the correct impact location, the estimated force time history will closely resemble the actual impact force, which is very concentrated and ordered. In comparison, the estimated force time history at other locations will be much less ordered, more dispersed, and more random. Therefore, the estimated force time history with the lowest entropy most likely corresponds to the actual location of impact.

The mathematical definition of entropy is based on a set of N possible outcomes, x_i , with probabilities $p(x_i)$. In this case, the probability distribution used is a categorical

distribution with the N possible outcomes corresponding to the signal amplitude falling into one of N possible ranges. The entropy, h , is computed as follows:

$$h = \sum_i^N -p(x_i)\log_2(p(x_i)) \quad (3)$$

The maximum value that the entropy may take is $\log_2(N)$, corresponding to a uniform random distribution, and the lowest value is zero, corresponding to a constant signal. In this application, N was chosen to be 200, but the impact identification algorithm was found to be fairly insensitive to the choice of N .

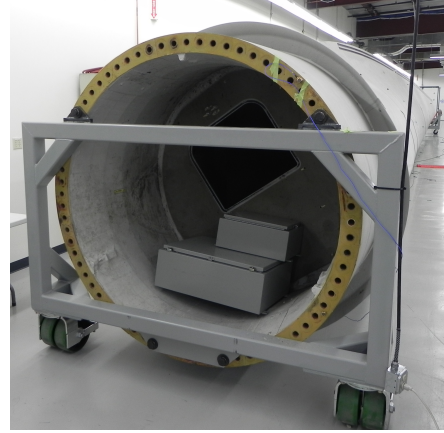
The most important use of the entropy value is selecting the most likely impact location, but the minimum entropy value is also useful in evaluating how well the impact force estimate meets the assumed impulsive shape. The lower the minimum entropy value is, the better the force estimate matches expectations of a simple impulsive load. The relationship between the minimum entropy value and the quality of the force estimate will be evaluated with the experimental results of this study.

3. Experimental Setup

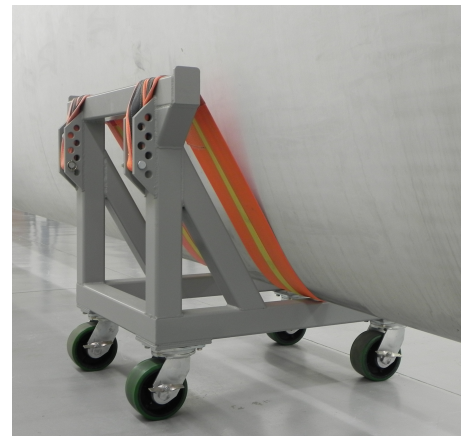
This impact identification technique was tested on a commercial wind turbine blade from a 1.6MW turbine. The blade was damaged in a lightning strike, and was delaminated at the tip with a portion of the tip missing. The blade was fastened at the root of the blade to a steel fixture, and supported towards the end of the blade with nylon straps. Figure 1 shows the blade and boundary conditions.

Five tri-axial accelerometers were mounted to the blade to test the influence of sensor placement on the accuracy of impact identification. Accelerometer 1 is a PCB 356T18, an ICP triaxial accelerometer with nominal sensitivity of 1000mV/g. Accelerometers 2-5 are Silicon Designs 2460-050 DC coupled piezoresistive triaxial accelerometers with nominal sensitivities of 80mV/g. A grid of 130 impact locations was marked on the section of the blade between the root and the support. The vertical spacing between points was approximately 0.36m, and the horizontal spacing was roughly 0.91m. The sensor and impact locations are shown in Figure 2.

To create the frequency response function model of the blade, modal impact testing was carried out using a 5.5kg modal sledge hammer, model PCB 086D50. Peak force amplitude for these impacts ranged from 542.2lbf to 2469.3lbf, with a mean value of 1205.4lbf and a standard deviation of 371.5lbf. The bandwidth of excitation, as measured by the first frequency where the amplitude of the force spectrum drops to one tenth the maximum



(a)



(b)

Figure 1. Photographs of test specimen, showing (a) attachment at the blade root, and (b) second blade support

amplitude, ranged from 101.5Hz to 281.5Hz, with a mean bandwidth of 174Hz, and a standard deviation of 31.5Hz. Testing was conducted with ten impacts per point, sampled at 2560Hz for a duration of 2 seconds per impact. Frequency response functions were estimated with the H1 estimator.

To test impact identification accuracy, a validation data set was collected with two impacts per point. The impact identification algorithm was applied to response data, and the estimated location and impact magnitude were compared to the known values to evaluate performance.

4. Results

In order to test the performance of the impact identification algorithm on the blade, the response data from each validation impact was passed through the algorithm, and the estimated location and maximum force level was recorded. Two key metrics will be used to evaluate the

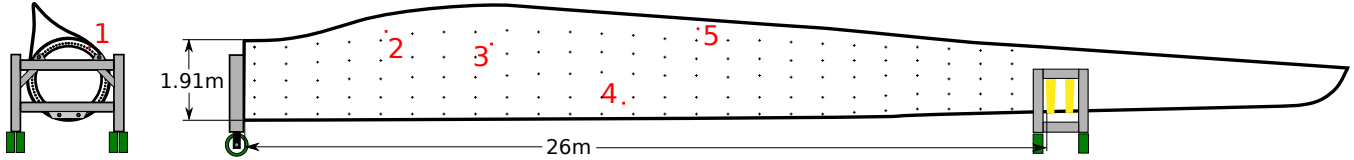


Figure 2. Illustration of the blade with approximate dimensions, sensor locations (enumerated in red), and impact locations (marked in black)

accuracy of the estimate: 1) the location identification accuracy, that is, how many of the validation impacts were correctly located, and 2) the magnitude of the peak force error, that is, the absolute value of the difference between the estimated and measured peak force relative to the measured peak force value.

To evaluate how sensor configurations affected the impact identification accuracy, the data from each of the five accelerometers was used individually to perform these validation simulations. Although the data for these sensors was collected simultaneously, only one sensor is used at a time in these validation tests. Accuracy is evaluated when data from all three measurement directions are used, when data from two of the three measurement directions are used, and when data from a single measurement direction are used.

The results of the validation simulation using all three response channels per sensor are summarized in Table 1. Regardless of the sensor location, 100% of impacts were accurately located. The accuracy of the impact force magnitude estimates was also fairly consistent between sensor locations. The peak force identification error was biased towards underestimating the peak magnitude of the impact force by an average of 0.68%. The fifth sensor, which was placed the furthest towards the blade tip and closest to the trailing edge, performed the best of the tested locations. The force estimates using the fifth sensor had a median error of 3.3%, with 75% of the impact forces estimated within 5.6% of the true peak force value, and a maximum error of 21.2%. The sensor with the lowest force accuracy was the fourth sensor, which was located closer to the root of the blade and close to the leading edge of the blade. The force estimation error for the fourth sensor had a median value of 4% and a maximum error of 35.8%.

From these results, the force accuracy shows no significant dependence on the distance from the sensor. Figure 3 is a scatter plot of the force error plotted against distance from the sensor, showing the results of validation tests using each of the available sensors. This plot illustrates the independence of the force accuracy on the distance from the sensor, even for very large distances. Most of the largest force estimation errors that were observed

Table 1. Impact Identification Performance Using Each Triaxial Accelerometer

Sensor	Force Estimation Error (%)				
	Quartile			Mean	Max
	1	2	3		
1	1.7	4.1	6.4	4.8	27.9
2	1.7	3.8	6.4	4.9	30.7
3	1.8	4.2	6.6	4.8	25.6
4	2.0	4.0	6.8	5.0	35.8
5	1.6	3.3	5.6	4.2	21.2

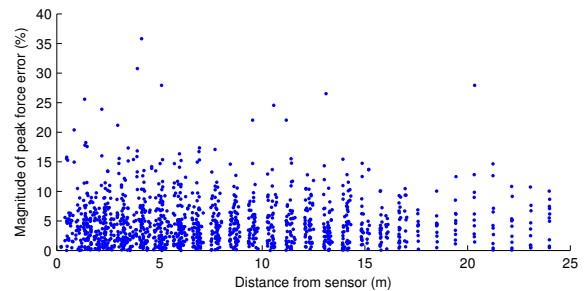


Figure 3. Force estimation error vs. distance from sensors for all combinations of sensor and impact location

were at locations relatively close to the sensor, but this fact is probably in part due to the larger number of points that are an intermediate distance from the sensor than those very distant. Other impact force identification techniques have shown a linear increase in error with distance from the sensor (Seydel & Chang, 2001), so the fact that distance and accuracy are largely uncorrelated in this instance is significant.

The same type of validation test was repeated with only two of the three response directions used, with the response data in the axial direction ignored. Using this subset of the data produces results very similar to those when all three response channels per sensor are used. The results are detailed in Table 2. Most of the mean errors are marginally higher than when using all three channels, but the median errors and maximum errors are mostly lower. Based on these results, a bi-axial accelerometer could be used just as effectively as a tri-axial accelerometer, even on very large structures.

Table 2. Impact Identification Performance Omitting Data in the Axial Direction

Sensor	Force Estimation Error (%)				
	Quartile			Mean	Max
	1	2	3		
1	1.9	3.9	6.6	4.8	28.1
2	1.6	3.8	6.4	4.8	30.3
3	1.8	4.2	6.6	4.9	25.4
4	2.0	4.0	6.7	4.9	35.7
5	1.6	3.3	5.5	4.2	21.1

The validation simulation results show that entropy of the estimated force time histories is an effective measure to discriminate between the force at the actual impact location and the other erroneous force estimates. When using two or three response channels, every impact was correctly located, so the entropy value corresponding to the impact location was always the least. To better evaluate how effective the recreated force entropy is in discriminating between correct and incorrect locations, the recreated force entropy is compared between the actual impact locations and the other incorrect impact locations. The results from all of the three channel validation response simulations were considered, and histograms of the recreated force entropy values for correct and incorrect locations are shown in Figure 4. For this comparison and the following entropy discussion, the signals were discretized to 200 amplitude values. Therefore, a purely random signal would have $\log_2(200) = 7.64$ bits of entropy. This comparison of entropy value distributions shows that the recreated force entropy is a very effective discriminator between the correct and incorrect locations. There is very little overlap between the two distributions, the entropy of the incorrect locations is tightly distributed, and the values of the correct location entropy are much lower than those from the corresponding incorrect locations. When entropy values from one impact were considered, the value corresponding to the correct location was always more than 1.5 times the interquartile range of the other entropies, with some values more than 10 times the interquartile range below the other entropy values. This measure indicates that for this set of data, not only is the entropy for the correct location always lowest, it is always a clear outlier of the distribution.

Entropy of the recreated force time histories effectively locates impacts because the value characterizes how well the force estimate meets the assumption of an impulsive load. Therefore, noise and error in the force estimate that alters the shape of the recreated force signal would generally contribute to an increase in the entropy of the force estimate. To evaluate the extent that the entropy

of the recreated force time history is related to error in the force estimate, the force estimates were split into seven categories according to entropy value. Boxplots of the magnitude of force estimation error were plotted for each of these entropy ranges in Figure 5, along with a histogram showing the frequency of estimates within each of these entropy ranges. Statistical measures corresponding to each of these entropy ranges are detailed in Table 3.

Both the average bias and variance of the force estimation error are monotonically increasing with the entropy value of the estimated force. Both the mean error and standard deviation for the force estimates with entropy greater than four are more than three times the corresponding values for estimates with entropy less than 2.5. This result is important because with an understanding of how the recreated force entropy and force error are related, the uncertainty in a force estimate can be characterized based on the entropy value for that estimate.

To further investigate the quantification of impact load uncertainty based on estimated force entropy, empirical cumulative distributions of the magnitude of impact force estimation error were investigated. These distributions, shown in Figure 6, indicate the increasing uncertainty and higher force estimation error for higher entropy forces. Another important feature of these distributions is that the distribution based on all force estimates is a poor indicator of the uncertainty of force estimates with high or low entropy values. Categorizing force estimates based on recreated force entropy better characterizes the uncertainty in that force estimate.

When considering all force estimates, 95% of validation tests showed a peak force estimation error of less than 12.6%. In contrast, 95% of estimates with entropy of less than 2.5 bits were accurate within 5.5%, while the 95th percentile level was 22% for force estimates with more than 4 bits of entropy. Therefore, the uncertainty for force estimates in the lowest entropy range was significantly overstated by the distribution of all estimates, and the uncertainty for force estimates with the highest entropy was significantly understated by the distribution of all estimates.

5. Conclusions

The entropy-based impact identification technique applied here was able to identify the location and magnitude of impact loads applied to a commercial wind turbine blade using a single sensor regardless of sensor location. Impact force identification accuracy was independent of the proximity to the sensor, enabling even very large structures like this one to be monitored with very few sensors.

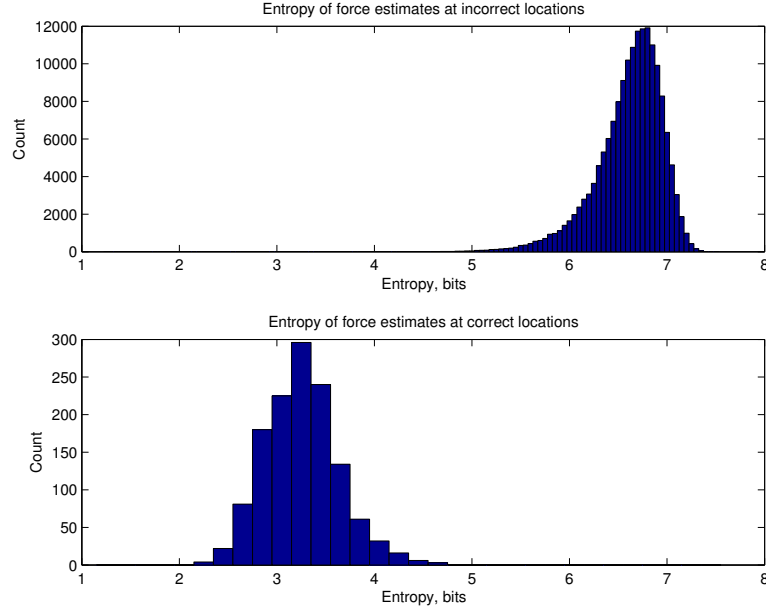


Figure 4. Histograms showing the distribution of entropy values for force estimates corresponding to incorrect locations (top) and correct locations (bottom)

Table 3. Peak force estimation error statistics corresponding to estimated force entropy

Entropy Range (bits)	Count	Magnitude of Peak Force Error (%)				
		Quartile			Mean	Standard Deviation
		1	2	3		
0 - 2.5	21	0.38	1.54	3.06	2.04	1.93
2.5 - 2.8	114	1.56	2.80	4.76	3.51	2.88
2.8 - 3.1	307	1.38	3.22	5.30	3.97	3.32
3.1 - 3.4	443	1.89	4.09	6.22	4.72	3.64
3.4 - 3.7	275	2.04	4.27	7.13	5.28	4.86
3.7 - 4	93	3.40	5.19	7.56	6.43	5.05
>4	47	3.03	4.3	8.87	6.97	6.19

The measure of recreated force entropy discriminates between force estimates from correct and incorrect locations very well, with the entropy at the correct location always being a statistical outlier. The value of the minimum recreated force entropy was shown to be a good indication of the uncertainty of that estimate. When categorizing the impact force estimates based on entropy values, the bias and variance of the peak force estimation errors monotonically increased with increasing entropy values. Comparing the 95th percentile force estimation accuracy levels between these entropy ranges showed that the uncertainty in force accuracy was more precisely identified when force estimates were categorized by entropy.

Identifying impact loads on large composite structures could significantly lower the associated inspection and repair costs by enabling condition based maintenance

rather than scheduled wide area inspections and unscheduled repairs when damage progresses unexpectedly. This impact identification technique allows for minimal sensing configurations, and the method of characterizing the uncertainty of these estimates allows these condition based maintenance decisions to be well informed.

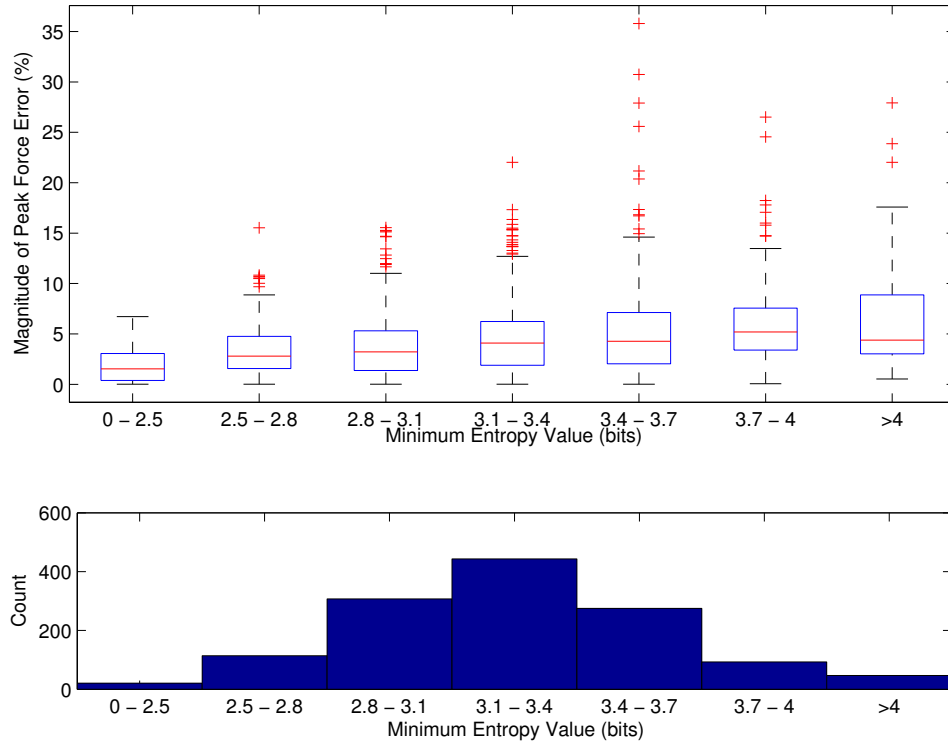


Figure 5. Relationship between impact force identification error and entropy of the force estimate

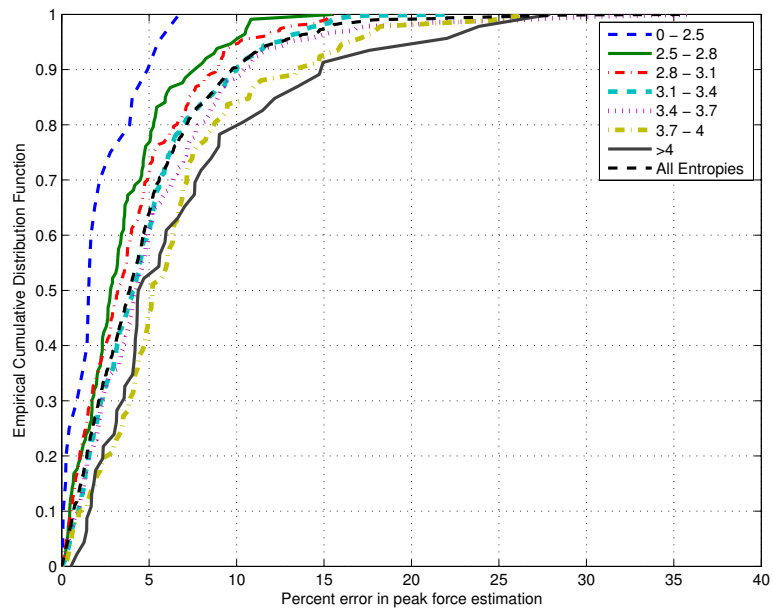


Figure 6. Empirical cumulative distributions of peak force estimation error for force estimates of varying entropy

Acknowledgment

The author would like to acknowledge support from Sandia National Laboratories through a graduate fellowship in the Sandia Campus Executive Fellowship Program.

References

- Adams, D., White, J., Rumsey, M., & Farrar, C. (2011). Structural health monitoring of wind turbines: method and application to a HAWT. *Wind Energy*, *14*(4), 603–623.
- Budde, C. (2010). *Impact force identification for composite helicopter blades using minimal sensing* (Unpublished master's thesis). Purdue University.
- Budde, C., Yoder, N., Adams, D., Meckl, P., & Koester, D. (2009). Impact detection for fiberglass composite rotor blade..
- Cripps, D. (2011). The future of blade repair. *Reinforced Plastics*, *55*(1), 28–32.
- Hahn, B., Durstewitz, M., & Rohrig, K. (2007). Reliability of wind turbines. In *Wind energy* (pp. 329–332). Springer.
- Hayman, B., Wedel-Heinen, J., & Brondsted, P. (2008). Materials challenges in present and future wind energy. *Warrendale: Materials Research Society*.
- H. Inoue, J. H., & Reid, S. (2001). Review of inverse analysis for indirect measurement of impact force. *Applied Mechanics Reviews*, *54*, 503.
- Hu, N., Matsumoto, S., Nishi, R., & Fukunaga, H. (2007). Identification of impact forces on composite structures using an inverse approach. *Structural Engineering and Mechanics*, *27*(4), 409–424.
- Inoue, H., Kishimoto, K., Shibuya, T., & Koizumi, T. (1992). Estimation of impact load by inverse analysis: Optimal transfer function for inverse analysis. *JSME International Journal. Ser. 1, Solid Mechanics, Strength of Materials*, *35*(4), 420–427.
- Seydel, R., & Chang, F. (2001). Impact identification of stiffened composite panels: Ii. implementation studies. *Smart Materials and Structures*, *Vol 10*, 370-379.
- Stites, N. (2007). *Minimal-sensing passive and semi-active load and damage identification techniques for structural components* (Unpublished master's thesis). Purdue University.
- Stites, N., Escobar, C., White, J., Adams, D., & Triplett, M. (2007). Quasi-active, minimal-sensing load and damage identification and quantification techniques for filament-wound rocket motor casings. In K. Tribikram (Ed.), (Vol. 6532, p. 65321E). SPIE. doi: 10.1117/12.715789
- Veritas, D. (2006). Design and Manufacture of wind turbine blades. *Offshore and Onshore Wind Turbines*, *1*.
- Wang, B., & Chiù, C. (2003). Determination of unknown impact force acting on a simply supported beam. *Mechanical Systems and Signal Processing*, *17*(3), 683–704.
- Yoder, N., & Adams, D. (2008). Multidimensional sensing for impact load and damage evaluation in a carbon filament wound canister. *Smart Materials and Structures*, *Vol. 66* (7), 756-763.